

A theory of the dynamics of DNA loop initiation in condensin/cohesin complexes

Bhavin S. Khatri*

Department of Life Sciences, Imperial College London,
Silwood Park, Ascot, SL5 7PY, United Kingdom
The Francis Crick Institute, 1 Midland Road, London, NW1 1AT, United Kingdom

*To whom correspondence should be addressed; E-mail: bkhatri@imperial.ac.uk

The structural maintenance of chromosome complexes exhibit the remarkable ability to actively extrude DNA, which has led to the appealing and popular “loop extrusion” model to explain one of the most important processes in biology: the compaction of chromatin during the cell cycle. A potential mechanism for the action of extrusion is the classic Brownian ratchet, which requires short DNA loops to overcome an initial enthalpic barrier to bending, before favoured entropic growth of longer loops. We present a simple model of the constrained dynamics of DNA loop formation based on a frictional worm like chain, where for circular loops of order, or smaller than the persistence length, internal friction to bending dominates solvent dynamics. Using Rayleigh’s dissipation function, we show how bending friction can be translated to simple one dimensional diffusion of the angle of the loop resulting in a Smoluchowski equation with a coordinate dependent diffusion constant. This interplay between Brownian motion, bending dissipation and geometry of loops leads to a qualitatively new phenomenon, where the friction vanishes for bends with an angle of exactly 180 degrees, due to a decoupling between changes in loop curvature and angle. Using this theory and given current parameter uncertainties, we tentatively predict mean first passage times of between 1 and 10 seconds, which is of order the cycle time of ATP, suggesting spontaneous looping could be sufficient to achieve efficient initiation of looping.

Introduction

A fundamental feature of all life is the faithful replication and segregation of DNA into daughter cells during cell division, where one of the key steps is the condensation and separation of sister chromatids (1); the protein complexes condensin and cohesin that are part of the family of structural maintenance of chromosome (SMC) complexes and are highly conserved throughout all domains of life, are essential

29 to this process and interact with DNA to regulate chromosome structure (2, 3). Condensin is known
30 to play a key role in the compaction of chromosomes during mitosis, while cohesin acts to bind
31 the sister chromatids together after DNA replication (4) and aids in chromosome alignment during
32 cell division. Early electron micrographs showed the structure of mitotic chromosome consist of a
33 central scaffold with loops of chromatin emanating from this central core (5). There is still much not
34 understood about how these complexes act to achieve these compact structures and the separation
35 of sister chromatids, but SMC complexes have been observed in vitro to exhibit the ability to actively
36 extrude DNA into loops (6–9), which has formed the basis of the popular loop extrusion model
37 of chromosome compaction: if a number of condensins bind to DNA and extrude loops, this will
38 naturally lead to compaction of chromatin, with the condensins forming a backbone (1, 10, 11).
39 Although, there are a number of empirical measurements that the loop extrusion model fails to
40 capture (12) and there are a number of unanswered questions as to whether loop extrusion can in
41 vivo lead to chromosome compaction, due to small stalling forces of motor activity (6) and how
42 extrusion can occur in the face of nucleosome obstacles (8), SMC complexes show extrusion activity
43 in vitro, which is poorly understood at a mechanistic level.

44 SMC complexes are essentially ring shaped protein trimers (13); they comprise a pair of coiled-
45 coils which are bound to each other at their hinge domains, while the opposing end comprises the
46 ATPase head domains that dimerise by ATP binding and are linked together by a mostly unstructured
47 polypeptide called the kleisin subunit. Although, many of the molecular details remain to be firmly
48 established and the exact path of DNA within the SMC complex is not known (known as topological,
49 pseudo-topological and non-topological in the literature (7, 14–16)), a key feature for looping is that
50 DNA is constrained or bound to the complex at two contact points (Fig.1), which enable the loop to
51 grow. There are various models of how extrusion might occur, but the simplest is a classic Brownian
52 ratchet mechanism (9), where ATP hydrolysis causes unbinding of the head domains, allowing the
53 DNA freedom to diffuse by Brownian motion with constrained electrostatic interactions with the
54 head domains and additional protein domains known as HEAT repeat subunits, ; the idea is that on
55 re-binding of ATP if the loop has grown by diffusion then this motion has been ratcheted. Molecular
56 motors powered by Brownian ratchet mechanisms work by relying on diffusion in some asymmetric
57 potential, here for sufficiently long loops entropy will favour the growth of loops. However, for
58 initially short loops the growth will be disfavoured by the enthalpy of bending. It is an open and
59 important question whether Brownian motion would be sufficiently rapid for SMC complexes to
60 initiate extrusion of DNA by this mechanism, or require additional force generation mechanisms to
61 drive initial loop growth.

62 From a physics perspective, the generic problem is one of the Brownian motion of a semi-flexible
63 polymer loop through an aperture whose size is of order the persistence length. Although, there has
64 been much theoretical (17, 18) and empirical work (19, 20) on the problem of DNA cyclisation, which
65 studies the rate that short lengths of DNA find their ends, this is not directly relevant to looping
66 within SMC complexes, as the constraints on DNA are different and the contour length of the loop
67 can grow. These theoretical studies also ignore the role of internal friction, which is dynamical
68 resistance to changing conformation due to internal energy barriers (21–23); it is well known from
69 Kuhn's theorem (21, 24) that for flexible polymers internal friction due to dihedral angle rotations
70 are negligible for long polymers and the longest wavelengths of their Rouse modes, and conversely
71 that for sufficiently short polymers they can be completely dominated by internal friction (25). The
72 internal friction of proteins (26–28), unfolded polypeptides (29), polysaccharides (23, 30) and single

73 stranded DNA (31) have all been measured empirically using a range of single molecule experimental
74 techniques. A key message from these studies is that many dynamical mechanical processes in
75 biology are far too slow to be explained if Stokes' friction with the solvent was the only source
76 of dissipation. In the case of semi-flexible or worm-like chain (WLC) polymers, measurements of
77 stretched polypeptides (29) and ssDNA (31) show that internal friction increases with tension F with
78 a power law $\sim F^{3/2}$ predicted by a frictional worm-like chain (FWLC), which includes dissipation
79 due to internal friction which opposes bending (29). The exact origin of bending friction is unclear,
80 but will be related to steric constraints between complex molecular potentials giving rise to a local
81 roughness that at a coarse-grained level gives an effective friction that opposes bending. Although,
82 the bending friction constant of dsDNA has not been measured, we a priori expect the same behaviour
83 as empirically determined for ssDNA and unfolded polypeptides.

84 In this paper, we address the fundamental theoretical question of Brownian loop growth by
85 calculating the mean first passage time to reach a critical loop size such that entropy dominates, in
86 the absence of any force generation mechanisms for loop growth. As we show, this is not a trivial
87 diffusion problem, since for short loops of DNA we expect frictional resistance to bending (internal
88 friction) within the polymer to dominate over Stokes' friction with the solvent. We formulate the
89 frictional worm like chain model to address this question and using Rayleigh's dissipation function
90 show that the constrained loop diffusion problem can be expressed as a 1 dimensional Smoluchowski
91 equation in the loop angle with coordinate dependent friction. This analysis demonstrates a new
92 physical phenomenon, which arises from an interplay between Brownian motion and loop geometry;
93 we find this effective angular friction vanishes at exactly 180 degrees, since at this exact angle,
94 infinitesimally, there is no change in curvature/bending of the loop and hence no bending friction.
95 Further, given this phenomenon, we predict that even with relatively large initial angles of the loop,
96 the mean first passage time to reach an entropically dominated loop is not significantly affected, and
97 is dominated by a relatively small range of angles greater than 180 degrees. Given uncertainties of
98 the exact parameter values – the internal friction to bending of double stranded DNA has not been
99 measured – we make tentative predictions based on reasonable assumptions and estimate that loop
100 initiation should take between 1 and 10 seconds. This time is of order the cycle time of ATP and
101 suggests that initiation by the purely spontaneous Brownian looping described could be sufficient for
102 efficient initiation of extrusion.

103 **Simple model of Brownian motion of DNA looping in SMC complexes**

104 Fig.1 shows a diagram representing the simple model of how DNA looping can occur by diffusion
105 in a SMC complex like condensin or cohesin, based on the Brownian ratchet model (9). The main
106 assumptions of the simple model are that 1) DNA is bound to the protein complex at two points
107 separated a distance d indicated with the small green circles, but free to slide frictionless through
108 the point and with no imposed constraint in angle and 2) the conformation of the loop between
109 the attachment points is an arc of a circle which has radius R (red line). After ATP hydrolysis and
110 coiled-coil head disengagement, one of the binding points to DNA correspond to an electrostatic
111 interaction with what is known as the head module (HEAT repeat subunit), which is bound to
112 one of the coiled-coils, while the other in reality only provides a steric constraint on DNA by the
113 same coiled-coil, but potentially constrained laterally by a kink in the coiled-coil referred to as the

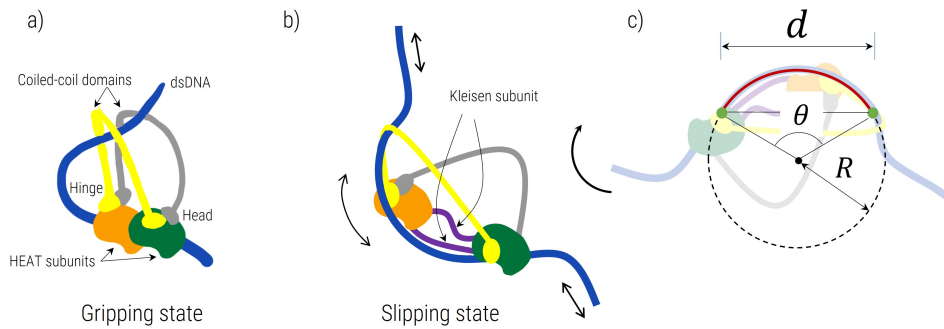


Figure 1: Diagram showing an idealisation of SMC complexes and DNA in gripping and slipping state (a & b) and c) how the looping of DNA is parameterised as an arc of a circle, where the d is the distance of the aperture constraining dsDNA and R is the radius and θ the angle of the loop. Note that although this diagram is based on the Brownian ratchet model (9) other models of extrusion can be represented by the same simple model shown in c) where the aperture d would correspond to a different distance.

114 elbow; their separation gives the effective aperture of size $d \approx 25\text{nm}$ through which the loop can
 115 grow (9, 32). These assumptions are reasonable as more compact DNA conformations are likely to
 116 be entropically and energetically disfavoured and unlikely to contribute significantly to random paths
 117 that lead to looping through the complex. However, there are a number of uncertainties about the
 118 exact molecular details (7, 14–16), and there may be alternative paths DNA can take as it loops
 119 (topological vs pseudo-topological vs non-topological); a key element is that post-hydrolysis DNA
 120 has freedom to diffusively slide (slipping state) – constrained to different degrees by electrostatic
 121 binding to the head and hinge domains (via the HEAT subunits) – and upon ATP binding with the
 122 head domains and DNA, any Brownian loop growth is ratcheted (9, 32). There are also very different
 123 models of how extrusion can occur within an SMC complex (33, 34), which broadly share the need
 124 for looping through an aperture, but where d would correspond to a different distance within the
 125 SMC complex. It should be further noted that this model does not include the initial search process
 126 and binding to DNA of the SMC complex, which means all estimates of mean first passage times
 127 below are lower bounds.

128 Given a circular loop we can write down the energy in terms of the radius R and the angle the loop
 129 subtends to its centre θ , given its persistence length ℓ_p : $U = \frac{k_B T \ell_p \theta}{2R}$. However, our simplification
 130 of the DNA strand being bound at both attachment points allows us to write down the radius in
 131 terms of the distance d and the angle θ , $R = \frac{d}{2 \sin(\theta/2)}$, and so the energy of the loop as a function
 132 of θ only:

$$U(\theta) = \frac{k_B T \ell_p}{d} \theta \sin(\theta/2) \quad (1)$$

133 where increasing θ corresponds to increased progress of looping and a larger radius. We can now
 134 characterise the looping as a Brownian walk in the variable θ in a potential landscape given by $U(\theta)$,
 135 which is plotted in Fig.2a in units of $k_B T$ for $d = 25\text{nm}$ and $\ell_p = 50\text{nm}$, where we see that maximum

136 energy of a loop occurs at around $\theta \approx 4$ radians or 230° .

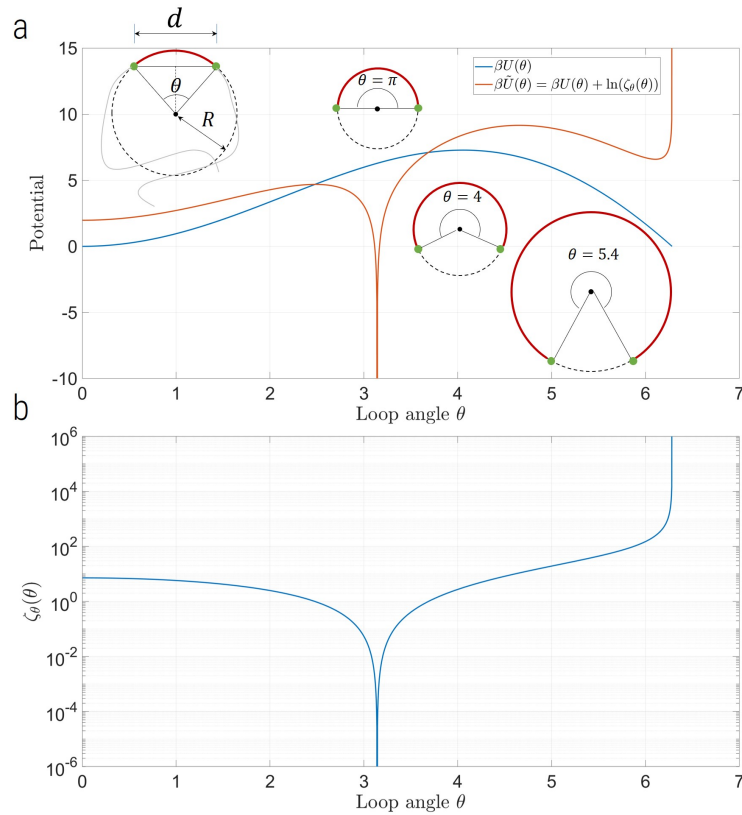


Figure 2: a) Potential energy $\beta U(\theta)$ (blue line) and the effective dynamical potential $\beta \tilde{U}(\theta) = \beta U(\theta) + \ln(\zeta_\theta(\theta))$ (red line) as a function of θ , where the latter incorporates the effect of internal friction in the dynamics of the loop. Note that the dynamic potential does not affect the Boltzmann distribution of angles which is still given by $U(\theta)$. The diagrams show the geometry of the DNA loop constrained to a distance d at two freely sliding attachment points, and also the relative loops sizes for different angles of $\theta = \pi$ (minimum friction), $\theta = 4$ (maximum internal energy) and $\theta = 5.4$, which corresponds to when the contour length of the loop $L = 3\ell_p$ and when the loop will tend to adopt non-circular conformations. b) Effective angular friction of a loop $\zeta_\theta(\theta)$ as a function of θ , showing vanishing friction at $\theta = \pi$ radians due the decoupling with changes in curvature at this angle.

137 The diffusion problem can be represented by the Smoluchowski equation:

$$\frac{\partial p(\theta, t)}{\partial t} = \frac{\partial}{\partial \theta} \left(\frac{k_B T}{\zeta_\theta(\theta)} \frac{\partial p(\theta, t)}{\partial \theta} + \frac{p(\theta, t)}{\zeta_\theta(\theta)} \frac{\partial U(\theta)}{\partial \theta} \right) \quad (2)$$

138 where $p(\theta, t)$ is the time-dependent probability density function of the angle θ as a function of time
 139 t and where the friction coefficient $\zeta_\theta(\theta)$ is the effective coarse grained opposition to motion to
 140 changes in the angular velocity $\dot{\theta}$, which as we will show is in general a function of the coordinate

141 θ . The possible contributions to this effective angular friction are solvent dynamics in the nucleus
 142 and/or internal friction within the DNA, which dynamically opposes changes in conformation.

143 The natural model for the dynamics that encompasses both types of friction is the frictional
 144 WLC (29, 35), which is a model of semi-flexible polymer dynamics, which adds a term to the WLC
 145 model (36–38) that penalises changes in conformation that have rapid changes in curvature, as
 146 expressed by the following Langevin equation (35):

$$\zeta_s \frac{\partial \mathbf{R}(s,t)}{\partial t} + \zeta_B \frac{\partial}{\partial t} \frac{\partial^4 \mathbf{R}(s,t)}{\partial s^4} + \kappa_B \frac{\partial^4 \mathbf{R}(s,t)}{\partial s^4} = \mathbf{f}(s,t) \quad (3)$$

147 where $\zeta_s \approx 6\pi\eta$ is a solvent friction per unit length (η is the solvent viscosity), ζ_B is the bending
 148 friction constant and $\kappa_B = k_B T \ell_p$ is the bending elastic constant and $f(s,t)$ is a spatially and
 149 temporally white noise term whose moments follow from the fluctuation dissipation theorem. A
 150 normal mode analysis shows the relaxation τ_q of different modes has a mode- and length-dependent
 151 contribution to the relaxation which arises from solvent dynamics, whilst there is a mode- and length-
 152 independent contribution from internal frictional processes, since both internal friction and bending
 153 elasticity are coupled to curvature, they give the same dispersion relation with mode number:

$$\tau_q = \frac{\zeta_s}{\kappa_B q^4} + \frac{\zeta_B}{\kappa_B} \quad (4)$$

154 where q is the wavenumber of the mode. Comparing these two contributions for the relaxation of
 155 loops, whose contour length is of order the persistence length, then internal friction dominates the
 156 dynamics when $\zeta_B \gg \zeta_s (\ell_p/2\pi)^4$; given $\ell_p = 50\text{nm}$ and $\zeta_s = 6\pi\eta \approx 10^{-5}\mu\text{g}/(\text{nm msec})$, we find
 157 $\zeta_B \gg 0.1\mu\text{g}\text{nm}^3/\text{msec}$. If we treat the semi-flexible polymer as an viscoelastic rod with an effective
 158 internal friction per unit length ζ_i , then simple arguments show that the bending friction should
 159 scale as $\zeta_B = \zeta_i r^4$, with r is the radius of the rod (35). Although ζ_B has not been measured for
 160 dsDNA, AFM experiments have estimated the bending friction for ssDNA as $\zeta_B \approx 11\mu\text{g}\text{nm}^3/\text{msec}$
 161 (31) and $\zeta_B = 0.3\mu\text{g}\text{nm}^3/\text{msec}$ for an unfolded polypeptide chain (29), which give an estimate
 162 of $\zeta_i = 176\mu\text{g}/\text{msec}/\text{nm}$ and $\zeta_i = 187.5\mu\text{g}/\text{msec}/\text{nm}$, respectively. The consistency of these two
 163 estimates suggests that the local energy barriers or the local roughness of potentials that determine
 164 the effective internal viscosity of both ssDNA and unfolded polypeptides are similar, at least to order
 165 of magnitude, and so if we take $\zeta_i \approx 180\mu\text{g}/\text{msec}/\text{nm}$, then the internal friction bending constant
 166 of dsDNA will be $\zeta_B \approx 180\mu\text{g}\text{nm}^3/\text{msec}$, which means for short loops of order a persistence length
 167 in contour length, internal friction will dominate and we only need consider this contribution to
 168 the Brownian motion of the loops. Alternatively, the double-stranded ladder structure of dsDNA
 169 may have a peculiar internal bending friction profile, which is not well approximated by a uniform
 170 viscoelastic rod, so at the other extreme we would expect dsDNA to have at least the internal friction
 171 of two strands of ssDNA acting in parallel, which would give twice the internal friction of ssDNA:
 172 i.e. $\zeta_B \approx 22\mu\text{g}\text{nm}^3/\text{msec}$, which is still comfortably in the regime where internal friction dominates
 173 solvent dynamics.

174 Now as the loop angle performs a random walk the internal friction mediating this is related to the
 175 changes in curvature and so we need a way of calculating the coupling between these processes – in
 176 other words we want to translate a bending friction constant ζ_B into an effective angular friction ζ_θ .
 177 This can be done by using the Rayleigh dissipation function of the DNA loop; within a Lagrangian
 178 formulation of mechanics, this in general is the dissipation rate of a system expressed in terms of the

179 squared velocities and the friction constant of the system, and so by using the relationship between
 180 the curvature of the loop $\kappa = 1/R = 2 \sin(\theta/2)/d$ and θ , we can derive an expression for the
 181 effective angular friction ζ_θ . The Rayleigh dissipation function of the DNA strand is:

$$182 \quad \mathcal{D} = \frac{\zeta_B L}{2} \left(\frac{d\kappa}{dt} \right)^2 \quad (5)$$

$$183 \quad = \frac{\zeta_B L}{2} \left(\frac{d\kappa}{d\theta} \frac{d\theta}{dt} \right)^2 \quad (6)$$

$$184 \quad = \frac{\zeta_B L}{2} \left(\frac{d\kappa}{d\theta} \right)^2 \left(\frac{d\theta}{dt} \right)^2 \quad (7)$$

$$185 \quad = \frac{\zeta_\theta}{2} \left(\frac{d\theta}{dt} \right)^2 \quad (8)$$

$$186 \quad (9)$$

187 where L is the contour length of the loop between the points separated by d . This result means the
 188 effective angular friction of the loop is

$$189 \quad \zeta_\theta = \zeta_B L \left(\frac{d\kappa}{d\theta} \right)^2 \quad (10)$$

$$190 \quad = \zeta_B \frac{d\theta}{2 \sin(\theta/2)} \frac{\cos^2(\theta/2)}{d^2} \quad (11)$$

$$191 \quad = \frac{\zeta_B \theta \cos^2(\theta/2)}{2d \sin(\theta/2)} \quad (12)$$

192 where we have used the fact that $L = R\theta$. We see that once translated to θ space the effective
 193 friction of the random walk has a very strong θ dependence, as plotted in Fig.2b, which shows in fact
 194 that the friction vanishes at exactly $\theta = \pi$ and diverges for $\theta = 2\pi$. We can understand both these
 195 phenomenon in geometric terms; given the constraint that the loop emerges from an aperture of size
 196 d , when $\theta \rightarrow \pi$ radians, small infinitesimal changes in the angle do not affect the radius of the loop,
 197 which means the curvature is unaffected and the friction must vanish, whilst the converse occurs as
 198 $\theta \rightarrow 2\pi$ radians, where small changes in the angle lead to a very large changes in the size of the
 199 loop and so rapid changes in curvature, where in the exact limit, the radius of the loop must become
 200 infinite. Of course, a vanishing internal friction means that at angles close to 180 degrees Stokes'
 201 friction will become dominant, which nonetheless we expect to make a negligible contribution to the
 202 mean first passage time and we ignore this in this treatment.

203 In practice, in the latter case once the contour length of the loop is much greater than the persis-
 204 tence length, the loop will adopt a very non-circular conformation before the divergence is reached.
 205 If we assume that once the contour length reaches a factor α larger than the persistence length,
 206 non-circular looping becomes dominant then these considerations give an approximate expression for
 207 the critical angle at which this occurs as

$$\theta^* = \frac{2\pi\alpha\ell_p}{d + \alpha\ell_p}. \quad (13)$$

208 For $d = 25\text{nm}$, $\ell_p = 50\text{nm}$ and $\alpha = 3$, this gives $\theta^* = 5.4$ radians, or $\theta \approx 310^\circ$, so this would predict
 209 that loops remain reasonably circular, before degenerating into a more random configuration.

210 Mean first passage time for loop initiation

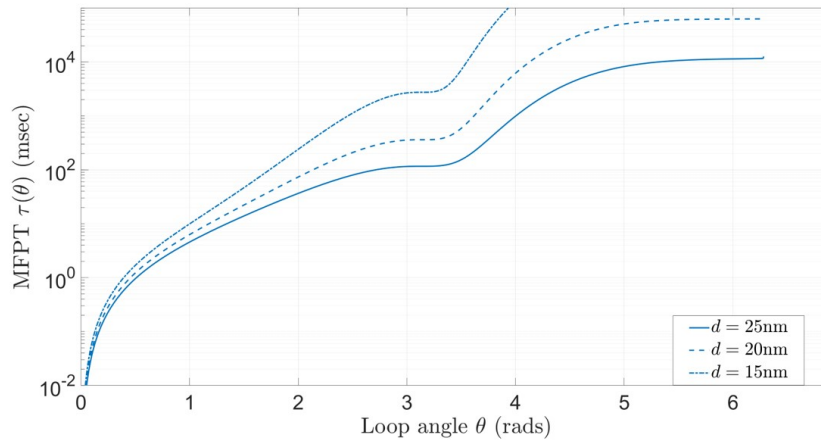


Figure 3: Mean first passage time $\tau(\theta)$ (Eqn.14) for loop to reach angle θ assuming $\ell_p = 50\text{nm}$, $d = 25\text{nm}$, $\zeta_B = 180\mu\text{g}\text{nm}^3/\text{msec}$.

211 Given the Smoluchowski Eqn.2, using the flux over population method (39), it is possible to
 212 show that the mean first passage time (MFPT) to reach an angle θ is given by the following exact
 213 expression:

$$\tau(\theta) = \beta \int_0^\theta d\theta' \zeta_\theta(\theta') e^{\beta U(\theta')} \int_0^{\theta'} d\theta'' e^{-\beta U(\theta'')} \quad (14)$$

214 where $\beta = 1/k_B T$. Although, various approximations can be obtained to evaluate this double
 215 integral, it is simple to numerically evaluate this instead, as shown in Fig.3 for different values of
 216 θ , where we take $\zeta_B = 180\mu\text{g}\text{nm}^3/\text{msec}$, the value we estimated for dsDNA; note that as $\zeta_\theta \sim \zeta_B$,
 217 which can come out of this integral, such that the MFPT $\tau \sim \zeta_B$, so that different assumptions
 218 about ζ_B give a proportional scaling. We see that the MFPT increases rapidly for increasing angle θ ,
 219 which diminishes as the loop approaches 180° at which there is an inflection point; this demonstrates
 220 the significant effect of the vanishing friction constant at $\theta = \pi$. For angles greater than 180° the
 221 MFPT again rapidly increases, begins to plateau for angles greater than $\theta = 5$ radians, and then
 222 divergences for angles very close to $\theta = 2\pi$, because of a diverging infinite friction, as observed above,
 223 although as discussed this divergence can be ignored, as in reality the chain will not be constrained
 224 to a circular conformation. For loop initiation dynamics in SMC complexes, the critical angle of
 225 interest is $\theta \approx \theta^* \approx 5.4$, where the loop remains approximately circular. However, we see that on a
 226 log-scale the mean first passage time has already nearly plateaued for this angle; in other words the

227 MFPT is strongly dominated by the time it takes to traverse a quite narrow range of angles, roughly
228 between 4 and 5.4 radians or 230° and 310° .

229 To understand this we note that the MFPT continues to increase rapidly even after the loop
230 has passed the angle of maximum energy ($\theta \approx 4$ radians), which can be explained because of
231 the still rapidly increasing internal friction of the loop; if we plot the effective dynamic potential
232 $\tilde{U}(\theta) = U(\theta) + k_B T \ln \zeta_\theta(\theta)$, which appears in the integrand of Eqn.14 for the MFPT, then we see
233 that it has a maximum at $\theta \approx 4.5$ radians and falls to more than $k_B T$ from the maximum at $\theta \approx 4$
234 radians and $\theta \approx 5.4$ radians. The angles which are within $k_B T$ of the maximum of the effective
235 potential represents the regions over which diffusion is effectively flat, and relatively slow, due to the
236 large internal friction at these angles.

237 Discussion

238 The observation of loop extrusion within SMC complexes, like cohesin and condensin, suggests that
239 such processes could be fundamental in the regulation of chromatin structure. Not least, it plays
240 a central role in the simple “loop extrusion” model of chromosome compaction during mitosis,
241 which is still an important and poorly understood fundamental biological process. Here we develop
242 the simplest first model of how loops can grow to sufficient size by Brownian motion within SMC
243 complexes, which is required for initiation of extrusion. We use this model of constrained Brownian
244 motion of dsDNA, to calculate the mean first passage time (MFPT) to quantify how quickly such
245 loops can form purely by the action of thermal Brownian motion, and so the degree to which loop
246 initiation is dynamically constrained.

247 As we show small loops with contour length of order the persistence length are very likely domi-
248 nated by internal friction to bending, rather than simple Stokes’ friction, which gives rise to a very
249 different and to date little studied polymer dynamics problem, in general, and in particular with
250 respect to understanding the dynamics of semiflexible polymers or worm-like chains like dsDNA. As
251 the DNA chain is constrained to emerge from a aperture of fixed size, we can formulate the Brownian
252 dynamics of looping using this frictional WLC model (29, 35), in terms of a 1D Brownian walk in the
253 angle of the loop. From these considerations we see that bending friction and geometry interplay
254 in a non-trivial way to determine the Brownian dynamics of loop growth, where friction vanishes at
255 exactly 180° and the overall MFPT is dominated by a narrow range of angles approximately centred
256 around a three-quarter circle (270°).

257 Evaluating the MFPT for $\theta = \theta^*$, we find $\tau \approx 10,000$ msecs or 10secs and as the MFPT
258 plateaus for angles approaching $\theta > \theta^*$ this estimate will be robust to order of magnitude given
259 our assumption that dsDNA is a uniform viscoelastic rod with internal bending friction constant
260 $\zeta_B = 180 \mu\text{gnm}^3/\text{msec}$. Alternatively, if we assume the internal bending friction constant is at least
261 the internal friction of two ssDNA strands in parallel, this would give $\zeta_B = 22 \mu\text{gnm}^3/\text{msec}$ (31),
262 which is an order of magnitude smaller and thus giving an order of magnitude smaller estimate of
263 $\tau \sim 1\text{sec}$. The range of angles which dominate the MFPT are unchanged as changing ζ_B just gives a
264 constant vertical shift in the effective dynamical potential $\tilde{U}(\theta)$. Empirical loop extrusion rates are of
265 order ~ 0.1 to 1 kbp/s (6–9), or ≈ 1 to $10 \ell_p/\text{s}$, and our result here suggests that the rate of initiation
266 of loops is at least $1/\tau = 0.1\text{s}^{-1}$ to 1s^{-1} , since this calculation ignores the time to find and then
267 bind DNA; although these two quantities need not agree, this suggests that loops are initiated at

268 roughly the same rate, or slower than, the rate at which they are extruded, once initiated. However,
269 more importantly the cycling time of ATP is of order $\sim 1\text{sec}$ (9) and so this would suggest that if
270 $\zeta_B \approx 180\mu\text{g}\text{nm}^3/\text{msec}$ corresponding to $\tau \sim 10\text{secs}$, then typically Brownian motion alone would
271 not quite be sufficient to generate a large enough loop in a single ATP cycle, although the probability
272 would not be small, and may require a few cycles. If on the other hand $\zeta_B \approx 22\mu\text{g}\text{nm}^3/\text{msec}$, which
273 corresponds to $\tau \sim 1\text{secs}$, then the probability of loop extrusion in a single cycle would be large.

274 There are other potential models of loop extrusion, such as the “tethered-inchworm” model (33)
275 and the segment capture model (34), which postulate extrusion through the SMC complex in an
276 unfolded conformation. These models do not discuss loop initiation and the simple model presented
277 here is equally applicable, but with $d > 25\text{nm}$ and a consequent expectation of a reduced mean first
278 passage time for looping.

279 There are a number of simplifications in this first model of Brownian looping applied to loop
280 initiation in SMC complexes. Firstly, it is clear that the binding of DNA to the hinge domain will not
281 be frictionless or unrestricted in angle. In addition, there could potentially be torsional constraints
282 on DNA on binding. Including some friction for sliding is relatively trivial and not affect the physical
283 phenomenon due to the interplay of loop bending and internal friction discussed, but would tend
284 to increase the quantitative estimates of MFPT. Regarding the constraints, given the electrostatic
285 and non-specific nature of binding to DNA it is likely that once ATP is hydrolysed and the complex
286 is in the slipping state any constraint on angle or torsion will be relatively weak. In any case, any
287 such constraints would tend to be somewhat relaxed some distance along the contour of the loop
288 and would likely give rise to a smaller effective aperture d , with a consequent increase in MFPT as
289 shown in Fig.3. We have also ignored the out of plane entropy of the DNA loop, which will have
290 some dependence on the contour length of the loop. However, as we have determined, the loop will
291 maintain a roughly circular conformation up until the critical angle θ^* , with fluctuations about this
292 mean conformation, such that entropic corrections will be logarithmic and relatively weak compared
293 to the role of internal friction of the loops.

294 Finally, there is a large literature on the cyclisation dynamics of short lengths of dsDNA, which
295 are of order a persistence length. The random walk problem of WLC like DNA finding its two
296 ends is very different to the question considered here, since the constraints are different and the
297 loop contour length can grow, although they both pertain to looping of DNA. Recent more careful
298 experiments (19, 20) have shown that cyclisation times are very much longer (~ 1 minutes) than
299 previously measured or predicted using the standard WLC. Despite the difference in constraints, the
300 calculation of the regimes where internal friction vs solvent friction are important for contour lengths
301 of dsDNA of order a persistence length are equally valid for the cyclisation problem and would suggest
302 the standard WLC model would significantly underestimate cyclisation times due to its neglect of
303 internal friction.

304 To summarise, we present a simple theory of Brownian loop growth in SMC complexes, where
305 internal friction to bending of double stranded DNA couples to the changing geometry of the loop to
306 determine the stochastic dynamics in a non-trivial way. For condensin/cohesin to act as a Brownian
307 ratchet, loops must first grow to sufficient size to overcome the initial enthalpic barrier; the model
308 remarkably predicts that friction for loop growth will vanish at 180° — with a corresponding plateau
309 in the MFPT — and that the MFPT for the loop to grow large enough that entropy favours its
310 growth is dominated loops that are roughly a three-quarter circle. This latter prediction conversely
311 means that loop initiation is largely insensitive to the initial angle of the bend induced in DNA in

312 the “gripping” state. Overall, we predict loop initiation times of order ~ 1 s to 10s, which is of order
313 the cycle time of ATP, suggesting loop initiation could initiate purely by Brownian motion without
314 the aid of additional active force generation mechanisms.

315 References

- 316 1. K. Nasmyth, *Annual Review of Genetics* **35**, 673 (2001).
- 317 2. T. Hirano, *Cell* **164**, 847 (2016).
- 318 3. F. Uhlmann, *Nature Reviews Molecular Cell Biology* **17**, 399 (2016).
- 319 4. C. H. Haering, A.-M. Farcas, P. Arumugam, J. Metson, K. Nasmyth, *Nature* **454**, 297 (2008).
- 320 5. J. R. Paulson, U. Laemmli, *Cell* **12**, 817 (1977).
- 321 6. M. Ganji, *et al.*, *Science* **360**, eaar7831 (2018).
- 322 7. I. F. Davidson, *et al.*, *Science* **366**, 1338 (2019).
- 323 8. Y. Kim, Z. Shi, H. Zhang, I. J. Finkelstein, H. Yu, *Science* **366**, 1345 (2019).
- 324 9. T. L. Higashi, G. Pobegalov, M. Tang, M. I. Molodtsov, F. Uhlmann, *eLife* **10**, e67530 (2021).
- 325 10. E. Alipour, J. F. Marko, *Nucleic Acids Research* **40**, 11202 (2012).
- 326 11. A. Goloborodko, M. V. Imakaev, J. F. Marko, L. Mirny, *eLife* **5**, e14864 (2016).
- 327 12. T. Gerguri, *et al.*, *Nucleic Acids Research* **49**, 1294 (2021).
- 328 13. S. Gruber, C. H. Haering, K. Nasmyth, *Cell* **112**, 765 (2003).
- 329 14. S. Cuylen, J. Metz, C. H. Haering, *Nature Structural & Molecular Biology* **18**, 894 (2011).
- 330 15. Y. Murayama, F. Uhlmann, *Nature* **505**, 367 (2014).
- 331 16. T. Kanno, D. Berta, C. Sjgren, *Cell Reports* **12**, 1471 (2015).
- 332 17. H. Yamakawa, W. H. Stockmayer, *The Journal of Chemical Physics* **57**, 2843 (1972).
- 333 18. K. B. Towles, J. F. Beausang, H. G. Garcia, R. Phillips, P. C. Nelson, *Physical Biology* **6**, 025001
334 (2009).
- 335 19. R. Vafabakhsh, T. Ha, *Science* **337**, 1097 (2012).
- 336 20. J. Jeong, H. D. Kim, *Nucleic Acids Research* **48**, 5147 (2020).
- 337 21. P. G. de Gennes, *Scaling Concepts in Polymer Physics* (Cornell University Press, 1985).
- 338 22. E. R. Bazúa, M. C. Williams, *The Journal of Chemical Physics* **59**, 2858 (1973).

- 339 23. B. S. Khatri, M. Kawakami, K. Byrne, D. A. Smith, T. C. B. McLeish, *Biophys J* **92**, 1825
340 (2007).
- 341 24. W. Kuhn, H. Kuhn, *Helv. Chim. Acta* **28**, 1533 (1945).
- 342 25. B. S. Khatri, T. C. B. McLeish, *Macromolecules* **40**, 6770 (2007).
- 343 26. A. Soranno, *et al.*, *Proceedings of the National Academy of Sciences of the United States of*
344 *America* **109**, 17800 (2012).
- 345 27. A. Borgia, *et al.*, *Nature communications* **3**, 1195 (2012).
- 346 28. D. d. Sancho, A. Sirur, R. B. Best, *Nature Communications* **5** (2014).
- 347 29. B. S. Khatri, *et al.*, *Faraday Discuss* **139**, 35 (2008).
- 348 30. M. Kawakami, *et al.*, *Langmuir* **20**, 9299 (2004).
- 349 31. M. Radiom, M. R. Paul, W. A. Ducker, *Nanotechnology* **27**, 255701 (2016).
- 350 32. T. L. Higashi, *et al.*, *Molecular Cell* **79**, 917 (2020).
- 351 33. M. H. Nichols, V. G. Corces, *Nature structural & molecular biology* **25**, 906 (2018).
- 352 34. J. F. Marko, P. DeLosRios, A. Barducci, S. Gruber, *Nucleic Acids Research* **47**, 6956 (2019).
- 353 35. M. G. Poirier, J. F. Marko, *Physical review letters* **88**, 228103 (2002).
- 354 36. M. Fixman, J. Kovac, *The Journal of Chemical Physics* **58**, 1564 (1973).
- 355 37. C. Bustamante, J. Marko, E. Siggia, S. Smith, *Science* **265**, 1599 (1994).
- 356 38. J. F. Marko, E. D. Siggia, *Macromolecules* **28**, 8759 (1995).
- 357 39. N. van Kampen, *Stochastic Processes in Physics and Chemistry* (North-Holland, 1981).

358 **Acknowledgements**

359 I thank Frank Uhlmann, Maxim Molodtsov and Tereza (Gerguri) Clarence for insightful discussions
360 and comments on the manuscript.

361 **Competing interests**

362 The author declares that they have no competing interests.

363 **Data and materials availability**